

## Europium-151 Mössbauer Spectra of Some Orthorhombic Perovskites

By Terence C. Gibb, Department of Inorganic and Structural Chemistry, The University, Leeds LS2 9JT

The  $^{151}\text{Eu}$  Mössbauer resonance in the orthorhombic perovskites  $\text{EuMO}_3$  ( $M = \text{Cr, Mn, Fe, or Co}$ ) is broadened by unresolved hyperfine effects. It is shown that this can be attributed to a quadrupole interaction with a coupling constant of  $e^2qQ_{\text{r}} \text{ ca. } -6.5 \text{ mm s}^{-1}$ . This value is in good agreement with the predicted value for  $\text{EuFeO}_3$  from a detailed crystal-field calculation. The induced magnetic exchange interactions which should occur at the europium ions in the solid solution  $\text{EuFe}_{0.8}\text{Cr}_{0.2}\text{O}_3$  have been found to be much smaller than predicted, and possible reasons for this are discussed.

THE ternary oxides containing the tripositive cations  $M$  (a first-row transition element) and  $M'$  (a lanthanide) of general formula  $M'\text{MO}_3$  are well known, and have a perovskite or distorted perovskite lattice. Although the ferromagnetic rare-earth iron perovskites,  $M'\text{FeO}_3$ , have been extensively studied by  $^{57}\text{Fe}$  Mössbauer spectroscopy, comparatively little attention has been given to the europium perovskites,  $\text{EuMO}_3$ , despite the ease with which the  $^{151}\text{Eu}$  Mössbauer resonance can be observed. This is no doubt a result of the diamagnetism of the  $^7F_0$  ground state of  $\text{Eu}^{3+}$ . Spectra have been reported previously<sup>1</sup> for  $M = \text{Al, Cr, Fe, and Co}$  at room temperature, and were described as single lines with unusually large half-widths in the region of  $3.5\text{--}4.0 \text{ mm s}^{-1}$  (compared to the theoretical natural width of  $1.31 \text{ mm s}^{-1}$  and typical experimental values in a range of other compounds of  $\geq 2.39 \text{ mm s}^{-1}$  using a source matrix of  $^{151}\text{SmF}_3$ ). It was remarked that in the 'perovskite structure, the rare-earth ion is probably in a highly symmetrical 12-co-ordinate site and should therefore give rise to no quadrupole splitting'. The fact that these compounds have a distorted lattice in which the geometry at the  $M'$  site is irregular was apparently overlooked.

Recent work in this laboratory<sup>2,3</sup> has shown the existence of transferred magnetic exchange interactions at  $\text{Eu}^{3+}$  ions in  $M''_2\text{EuRuO}_6$  ( $M'' = \text{Ca, Sr, or Ba}$ ) and in  $M''\text{Eu}_2\text{Fe}_2\text{O}_7$  ( $M'' = \text{Sr or Ba}$ ) which arise from the neighbouring magnetic ion ( $\text{Ru}^{5+}$  or  $\text{Fe}^{3+}$ ). These parallel the better known case of the rare-earth iron garnet,  $\text{Eu}_3\text{Fe}_5\text{O}_{12}$ . As both  $\text{EuCrO}_3$  and  $\text{EuFeO}_3$  are known to order magnetically, it was decided to look more closely at the broad lines in the  $\text{EuMO}_3$  perovskites to see whether magnetic and/or quadrupole hyperfine effects were involved.

### EXPERIMENTAL

Samples of  $\text{EuCrO}_3$ ,  $\text{EuMnO}_3$ ,  $\text{EuFeO}_3$ ,  $\text{EuCoO}_3$ , and the solid solutions  $\text{EuFe}_{0.8}\text{Al}_{0.2}\text{O}_3$  and  $\text{EuFe}_{0.8}\text{Cr}_{0.2}\text{O}_3$  were made by weighing out stoichiometric ratios of the appropriate high-purity oxides, grinding in a ball-mill, and firing in air to ca.  $1200^\circ\text{C}$ . Additional samples of  $\text{EuFeO}_3$  and  $\text{EuCoO}_3$  were made by the alternative method<sup>4</sup> of calcining the appropriate complex cyanide  $\text{EuM}(\text{CN})_6 \cdot x\text{H}_2\text{O}$  ( $M = \text{Fe or Co}$ ) at  $1000^\circ\text{C}$ , in the view that these would have a more closely controlled stoichiometry. The resultant products were characterised by X-ray diffraction data recorded with

a Philips diffractometer using nickel-filtered  $\text{Cu-K}\alpha$  radiation and compared with published data. All samples gave patterns characteristic of the orthorhombic perovskite with no other phases evident, and no significant differences were observed between corresponding ceramic and cyanide preparations.

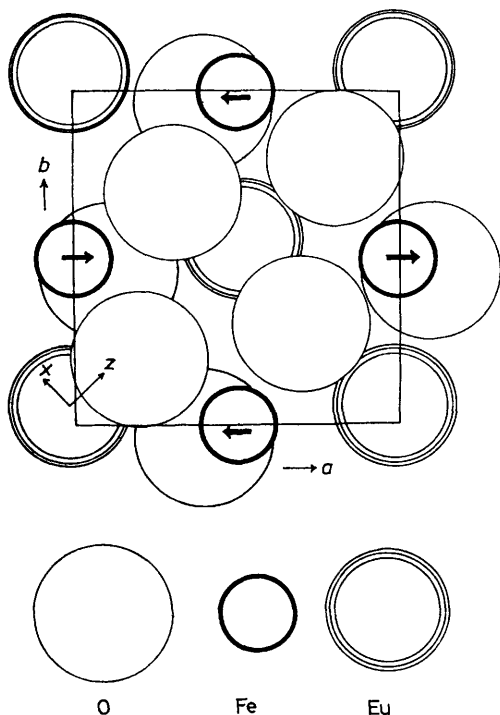
The  $^{57}\text{Fe}$  and  $^{151}\text{Eu}$  spectra were obtained at 85 or 295 K using established techniques and source matrices of  $^{57}\text{Co}$  (Rh) and  $^{151}\text{SmF}_3$  respectively. Accumulation time was usually ca. 7 d to achieve a good signal-to-noise ratio.

### RESULTS AND DISCUSSION

*Crystal Symmetry.*—The crystal structures of the rare-earth orthoferrites have been determined by Marezio *et al.*<sup>5</sup> The compound  $\text{EuFeO}_3$  belongs to the orthorhombic space group  $Pbnm$  ( $D_{2h}^{16}$ ) with  $a = 5.372$ ,  $b = 5.606$ ,  $c = 7.685 \text{ \AA}$ , and  $Z = 4$ . The  $\text{Eu}^{3+}$  sites have the point symmetry  $m$  ( $C_s$ ), and they lie in mirror planes normal to the  $c$  axis. The twelve-co-ordination to oxygen in the regular perovskite lattice has become severely distorted, and the  $\text{Eu-O}$  bond distances range from  $2.297$  to  $3.510 \text{ \AA}$ . There are eight nearest-neighbour iron sites in pairs (above and below the mirror plane) at  $3.127$ ,  $3.257$ ,  $3.383$ , and  $3.682 \text{ \AA}$ . The  $\text{Eu-O-Fe}$  bond angles are between  $81.7$  and  $115.0^\circ$ . A projection of the structure onto the mirror plane is shown in the Figure; only those iron and oxygen atoms immediately above and below the mirror plane containing oxygen and europium atoms are shown.

The magnetic structure of  $\text{EuFeO}_3$  at all temperatures and of all the rare-earth orthoferrites at high temperatures is well known,<sup>6</sup> and is frequently referred to by the notation  $\Gamma_4(F_z)$ . The strong iron-iron exchange interaction causes the spins to couple antiferromagnetically parallel to the  $a$  axis in a magnetic mode  $G_x$ . (The spin directions for the upper layer of Fe atoms in the Figure are shown as solid arrows, those for the lower layer being reversed.) However, this spin configuration is symmetry compatible with the mode  $F_z$  in which all the spins are parallel to the  $c$  axis, and consequently in the real lattice the spins are slightly canted to give a net ferromagnetic moment in the  $c$  direction. The canting angle in  $\text{EuFeO}_3$  is only  $8.0 \text{ mrad}$  ( $0.46^\circ$ ), and is effectively independent of temperature.<sup>7</sup>

*The Electric Field Gradient at  $\text{Eu}^{3+}$ .*—The  $^7F_0$  ground state for  $\text{Eu}^{3+}$  ( $4f^6$ ) is diamagnetic and does not give rise to an electric field gradient (e.f.g.). However, there are



Projection of the structure of EuFeO<sub>3</sub> on the *ab* plane. The spin directions in the upper layer are shown, those in the lower layer being reversed. The axes of the e.f.g. tensor at the Eu<sup>3+</sup> site are also shown

low-lying excited states,<sup>3</sup> the <sup>7</sup>F<sub>1</sub> state at approximately 520 K and the <sup>7</sup>F<sub>2</sub> state at 1540 K. If the crystalline field is non-cubic, then the resulting admixture into the ground state can produce a finite e.f.g., which is also temperature dependent as the excited states become thermally populated. This contribution is however smaller than a temperature-independent contribution from the lattice charges external to the europium atom.

The e.f.g. tensor can be written as equation (1) where

$$eq_{lm} = (1 - R)eq_{lm}^{(\text{val})} + (1 - \gamma_{\infty})eq_{lm}^{(\text{latt})} \quad (1)$$

$l, m = x, y, z$ . The first term derives from the electrons in the partially filled 4*f* shell which also produce a secondary effect on the closed inner shells expressed as the 'atomic' Sternheimer factor, *R*. The second term arises directly from all the ions surrounding the atom of interest, but is grossly affected by a distortion of the closed inner shells which is expressed as the 'lattice' Sternheimer factor,  $\gamma_{\infty}$ .

Since the crystal structure of EuFeO<sub>3</sub> is known accurately, the atomic co-ordinates can be used to obtain the summation over all ions in the lattice for the tensor  $eq_{lm}^{(\text{latt})}$  as equation (2) where  $Z_k$  is the charge on the ion

$$eq_{lm}^{(\text{latt})} = \sum_k \frac{Z_k}{4\pi\epsilon_0} \left( \frac{3r_{lk}r_{mk} - \delta_{lm}r_k^2}{r_k^5} \right) \quad (2)$$

at a distance  $r_k$  and  $r_{lk}, r_{mk}$  are the appropriate components along *l* and *m*, and  $\epsilon_0$  is the permittivity of a vacuum.

The calculation of  $eq_{lm}^{(\text{val})}$  in the case of a combined magnetic exchange interaction and a crystalline field for an Eu<sup>3+</sup> ion whose only symmetry is a mirror plane has been developed fully elsewhere<sup>3</sup> (in a discussion of SrEu<sub>2</sub>Fe<sub>2</sub>O<sub>7</sub>) and will only be summarised here. The e.f.g. tensor at the europium site must correspond to the mirror symmetry with one of the principal axes normal to the mirror plane (along the *c* axis) and the other two oriented at an arbitrary angle within the plane. If the magnetic exchange is negligible, the energy-level scheme for Eu<sup>3+</sup> ( $L = 3, S = 3$ ) can be calculated for the nine states  $|L, S, J, J_z\rangle$  of <sup>7</sup>F<sub>0</sub> + <sup>7</sup>F<sub>1</sub> + <sup>7</sup>F<sub>2</sub> using the Hamiltonian (3) where  $E_J$  is the energy of the unper-

$$\mathcal{H} = E_J + \mathcal{H}_{\text{cryst}} \quad (3)$$

turbed <sup>7</sup>F<sub>J</sub> state. The fact that the *f* orbitals are only weakly involved in chemical bonding means that  $\mathcal{H}_{\text{cryst}}$  can be described by a point-charge approximation more accurately than in Fe<sup>3+</sup> for example, but there remain several difficulties. Such calculations have been described in the literature<sup>8</sup> for the rare-earth iron garnets, and the effects of electronic shielding by closed shells are understood at least qualitatively.<sup>9</sup>

$\mathcal{H}_{\text{cryst}}$  is most conveniently written in the form (4)

$$\mathcal{H}_{\text{cryst}} = \sum_{n,m} B_n^m \langle J || \alpha_n || J' \rangle O_n^m \quad (4)$$

where  $O_n^m$  is an angular momentum operator,  $\langle J || \alpha_n || J' \rangle$  is the corresponding reduced matrix element, and  $B_n^m = (1/4\pi\epsilon_0)A_n^m \langle r^n \rangle$ . The coefficients  $A_n^m$  are proportional to summations over all lattice points in the crystal.<sup>3</sup> The radial expectation value  $\langle r^n \rangle$  is modified from the free-ion value of a 4*f* wavefunction  $\langle r^n \rangle_{4f}$  by a deformation of the closed electron shells, and this has been expressed<sup>9</sup> by the introduction of an additional 'shielding factor',  $\sigma_n$ , such that  $\langle r^n \rangle = (1 - \sigma_n) \langle r^n \rangle_{4f}$ . The matrix elements for  $A_n^m$  vanish when *n* is odd, and within the basis set <sup>7</sup>F<sub>0</sub> + <sup>7</sup>F<sub>1</sub> + <sup>7</sup>F<sub>2</sub> all terms with  $n \geq 6$  also vanish. For a Eu<sup>3+</sup> ion in a mirror plane (symmetry *m* or *C<sub>s</sub>*) there are only nine  $A_n^m$  terms which transform as *A'*, being  $A_0^0$  which is trivial and  $A_2^0, A_2^{\pm 2}, A_4^0, A_4^{\pm 2}, A_4^{\pm 4}$ . The values of  $A_n^m$  and hence  $B_n^m$  can be obtained directly by summation using the crystal-structure data.

The expressions for the operators  $O_n^m$  are very complicated, but are available in the literature,<sup>9</sup> and the matrix elements for the nine wavefunctions of <sup>7</sup>F<sub>0</sub> + <sup>7</sup>F<sub>1</sub> + <sup>7</sup>F<sub>2</sub> can then be evaluated<sup>3</sup> using standard if laborious methods. Diagonalisation gives the eigenvalues  $E_i$  and the eigenvectors  $|i\rangle$  for each of the *i* states. The tensor  $eq_{lm}^{(\text{val})}$  can then be evaluated for each electron level. The valence contribution to the e.f.g. tensor at a temperature *T* is then obtained by Boltzmann summation as equation (5),  $l, m = x, y, z$ .

$$eq_{lm}^{(\text{val})} = \sum_{i=1}^9 [eq_{lm}^i \exp(-E_i/kT)] / \sum_{i=1}^9 \exp(-E_i/kT) \quad (5)$$

The valence and lattice contributions to the e.f.g. tensor  $eq_{lm}$  are then summed, and the principal values

obtained by diagonalisation. The quadrupole contribution to the Mössbauer spectrum can then be expressed conventionally in terms of  $e^2qQ_g$ , the asymmetry parameter  $\eta$ , and three angles to give the orientation of the principal axis system relative to the crystal axes.

This calculation was carried out for  $\text{EuFeO}_3$ . The following numerical values were adopted: the  $\gamma$ -ray energy  $E_\gamma = 21.532$  keV; \* nuclear quadrupole moments  $Q_g = +1.14 \times 10^{-28}$  m<sup>2</sup> and  $Q_e/Q_g = +1.31$ ;  $(1 - \gamma_\infty) = 81$  (ref. 10); nuclear magnetic moments  $\mu_g = 1.5206$  mm s<sup>-1</sup> T<sup>-1</sup> and  $\mu_e/\mu_g = 0.7465$ ; expectation values for the  $4f$  electrons  $\langle r^2 \rangle = 0.83$  a<sub>0</sub><sup>2</sup>,  $\langle r^4 \rangle = 1.70$  a<sub>0</sub><sup>4</sup>, and  $\langle r^{-3} \rangle = 7.53$  a<sub>0</sub><sup>-3</sup> (ref. 11). Accurate experimental values for the  $\sigma_n$  coefficients are not available<sup>9,12</sup> and the values  $(1 - \sigma_2) = 0.4$  and  $(1 - \sigma_4) = 0.6$  were assumed, with  $(1 - R) = 0.8$ .

A summation over a sphere of radius 5 000 pm converged satisfactorily and gave the following results for the lattice contribution:  $e^2qQ_g$  (lattice) =  $-15.06$  mm s<sup>-1</sup>,  $\eta = 0.003$ ,  $V_{yy}$  normal to the mirror plane and parallel to the  $c$  axis,  $V_{zz}$  at 46° to the  $a$  axis in the  $ab$  plane (close to the  $a$  axis of the undistorted perovskite lattice). The  $B_n^m$  coefficients defined in the  $a, b, c$ , axis system were  $B_2^0 = -158$ ,  $B_2^2 = -21$ ,  $B_2^{-2} = 473$ ,  $B_4^0 = -37$ ,  $B_4^2 = -271$ ,  $B_4^{-2} = 924$ ,  $B_4^4 = -23$ , and  $B_4^{-4} = -1\ 935$  K.

The total e.f.g. is temperature dependent. At 4.2 K,  $e^2qQ_g = -7.83$  mm s<sup>-1</sup>,  $\eta = 0.11$ ,  $V_{zz}$  at 42° to the  $a$  axis, and  $V_{yy}$  along the  $c$  axis; at 100 K,  $e^2qQ_g = -7.66$  mm s<sup>-1</sup>,  $\eta = 0.11$ ,  $V_{zz}$  at 42° to the  $a$  axis; at 300 K,  $e^2qQ_g = -7.81$  mm s<sup>-1</sup>,  $\eta = 0.15$ ,  $V_{zz}$  at 44° to the  $a$  axis. Thus ignoring other effects such as thermal expansion of the lattice, the major effect of temperature is to produce small changes in  $e^2qQ_g$  (<20% below 500 K).

Adequate crystallographic data are not available for the other compounds studied here, but the calculation of the lattice term was repeated for all the rare-earth orthoferrites<sup>5</sup> from Pr to Lu to examine the self-consistency of the results, which in the event proved to be good. The value of  $e^2qQ_g^{\text{(latt)}}$  decreased steadily from  $-14.59$  mm s<sup>-1</sup> in  $\text{PrFeO}_3$  to  $-20.09$  mm s<sup>-1</sup> in  $\text{LuFeO}_3$ , in accord with the decreasing lattice parameter. The value of  $\eta$  decreased from 0.37 in  $\text{PrFeO}_3$  until  $V_{zz}$  changed from the  $c$  axis (Pr—Sm) to the  $ab$  plane (Eu—Lu), whereupon it increased steadily to 0.77 at  $\text{LuFeO}_3$ . The direction of  $V_{zz}$  remained in the  $ab$  plane but rotated from 37° to the  $a$  axis in  $\text{PrFeO}_3$  to 61° in  $\text{LuFeO}_3$ . These results are of course for  $\text{Eu}^{3+}$  ions doped into the  $\text{MFeO}_3$  lattices.

The results are not drastically affected by a different choice of the shielding parameters. For example, if we adopt the theoretical estimates<sup>13</sup> of  $(1 - R) = 0.884$ ,  $(1 - \gamma_\infty) = 62.38$ , and  $(1 - \sigma_2) = 0.314$ , the calculations for  $\text{EuFeO}_3$  at 4.2 K give  $e^2qQ_g = -8.66$  mm s<sup>-1</sup>,  $\eta = 0.08$ ,  $V_{zz}$  at 43° to the  $a$  axis, and  $V_{yy}$  along the  $c$  axis. Errors in the shielding constants contribute to an error in  $e^2qQ_g$  but have very little effect on the actual orientation of the e.f.g.

\* Throughout this paper:  $1 \text{ eV} \approx 1.60 \times 10^{-19} \text{ J}$ .

<sup>151</sup>Eu Mössbauer Data.—The <sup>151</sup>Eu spectra at 295 K of all the  $\text{EuMO}_3$  compounds were single but broad lines that on casual inspection appeared close to Lorentzian in shape. However, a least-squares fit of such a line-shape gave poor chi-squared values ( $\chi^2 > 1\ 200$  on 248 degrees of freedom) with linewidths of 3.19 (Cr), 2.91 (Mn), 3.41 (ceramic Fe), 3.27 (cyanide Fe), and 2.89 (Co) mm s<sup>-1</sup>. The percentage dip was ca. 12% in all cases. On the other hand the linewidth of hydrated europium nitrate was only 2.26 mm s<sup>-1</sup>. At 295 K, only the  $\text{EuFeO}_3$  is magnetically ordered ( $T_N = 662$  K), but  $\text{EuCrO}_3$  orders below  $T_N = 181$  K. At 85 K the linewidth in  $\text{EuCrO}_3$  had increased to 3.60 mm s<sup>-1</sup>. However, the increase can be accounted for at least in part by the increase in absorption cross-section with increasing recoilless fraction as the temperature is lowered. Small differences in cross-section between absorbers could also affect the relative linewidths, and the linewidth of  $\text{EuFeO}_3$  for a thinner sample (ca. 6% absorption) was 3.03 mm s<sup>-1</sup> at 300 K and 3.27 mm s<sup>-1</sup> at 85 K.

There is no immediate evidence to suggest that the <sup>151</sup>Eu resonance in  $\text{EuFeO}_3$  (or in  $\text{EuCrO}_3$  at 85 K) is significantly broadened by a magnetic exchange interaction. This is in fact compatible with the antiferromagnetic structure. Pairs of iron atoms on either side of the mirror plane containing the  $\text{Eu}^{3+}$  ions are mutually compensating in effect in the  $G_x$  structure, and it is only the  $F_z$  component which can produce a resultant magnetic field. If for the moment we take the observed magnetic flux density in  $\text{Eu}_3\text{Fe}_5\text{O}_{12}$  at 0 K of ca. 60 T from two nearest-neighbour iron atoms (*i.e.* ca. 30 T per nearest neighbour) as a typical order of magnitude, then the canting angle of 8.0 mrad for eight Fe nearest-neighbour spins would produce a flux density of only 1.9 T. This is much smaller than that of 11 T in  $\text{SrEu}_2\text{Fe}_2\text{O}_7$  at 0 K, and is probably below the practical limits of resolution. However, in the light of the data which follow for the solid-solution phases, it will be seen that this estimate is in any case too large.

The least-squares fitting of either a magnetic hyperfine or a quadrupole splitting causes a substantial reduction in the values of  $\chi^2$ . However, a detailed interpretation is not realistic for the following reasons. First, the source matrix of  $\text{SmF}_3$  is itself non-cubic, and therefore the source emission line may be slightly unsymmetrical. Secondly, the high absorption cross-section for <sup>151</sup>Eu means that saturation effects may be significant; this not only broadens the observed linewidth but can also cause distortions of the 'zero-thickness' quadrupole spectrum. Because, as we have seen, a magnetic splitting of any magnitude is unlikely, the spectra have been analysed on the basis of a single quadrupole splitting to compare the results obtained with those predicted by the crystal-field calculation. The numerical values obtained for 295 K were  $e^2qQ_g = -7.2$  (Cr),  $-5.6$  (Mn),  $-6.1$  (ceramic Fe),  $-6.6$  (cyanide Fe), and  $-6.5$  (Co) mm s<sup>-1</sup>, with  $\eta = 0.7, 1.0, 0.8, 0.9,$  and  $0.6$ , and linewidths of 2.25, 2.18, 2.72, 2.37, and 2.10 mm s<sup>-1</sup> respectively. The

sign and magnitude of  $e^2qQ_g$  for  $\text{EuFeO}_3$  is in good agreement with prediction. Similar values can be expected for the other compounds because of the similar ionic radii of the  $\text{M}^{3+}$  cations. The linewidths for all the compounds are also reasonable values. Unfortunately the spectra of both preparations of  $\text{EuFeO}_3$  are surprisingly symmetrical and suggest a large  $\eta$  value, which was not predicted. However, it is considered that the convolution of the absorption spectrum with an asymmetric source lineshape and with additional saturation effects could be partly responsible for this observation. In view of the uncertainties involved, the only conclusion which can be reliably drawn is that the spectra are compatible with a quadrupole interaction of  $e^2qQ_g$  ca.  $-6.5 \text{ mm s}^{-1}$  and with the predictions of the crystal-field model.

**Solid Solutions.**—The solid solution  $\text{EuFe}_{0.8}\text{Cr}_{0.2}\text{O}_3$  was examined at room temperature by  $^{57}\text{Fe}$  Mössbauer spectroscopy, and gave a broadened hyperfine pattern similar to that previously published<sup>14</sup> for  $\text{TbFe}_{0.8}\text{Cr}_{0.2}\text{O}_3$  in a detailed study of that phase. The material can

The close similarity of the values of  $e^2qQ_g$  in the  $\text{EuMO}_3$  compounds suggest that only minor variations will occur in the solid solutions. On this basis it is possible that some of the additional broadening can be attributed to magnetic exchange. Some computer fits for combined magnetic–quadrupole interactions were attempted with suitable constraints placed upon the latter. Although these calculations were unrealistic, they resulted in the conclusion that the flux density extrapolated to zero Kelvin,  $B_{\text{eff}}(0)$ , was  $\leq 2.0 \text{ T}$  with one or two chromium nearest neighbours.

One might have thought that the replacement of one  $\text{Fe}^{3+}$  ion in an antiferromagnetically coupled pair by a  $\text{Cr}^{3+}$  ion ( $S = \frac{3}{2}$ ) coupled ferromagnetically to the remaining  $\text{Fe}^{3+}$  ion ( $S = \frac{5}{2}$ ) would have resulted in a much larger exchange field than has been observed. A possible explanation can be found in the available data (see Table). The magnetic exchange constant  $\beta B^m(0)$  shows substantial variation from compound to compound. In the case of  $\text{Eu}_3\text{Fe}_5\text{O}_{12}$  it has been convincingly shown<sup>15</sup> that some 88% of the exchange interaction

Data for solid solutions

	$\text{Eu}_3\text{Fe}_5\text{O}_{12}$ *	$\text{Sr}_2\text{EuRuO}_6$	$\text{Ba}_2\text{EuRuO}_6$	$\text{SrEu}_2\text{Fe}_2\text{O}_7$	$\text{EuFeO}_3$
$B_{\text{eff}}(0)/\text{T}$	ca. 60	28	27	11	< 2
$\beta B^m(0)/\text{K}$	ca. 26	12	11	3	< 1
No. of M atoms	2 (4)	6	6	6	1–3
No. of O atoms	2 (4)	1	1	1	3
Eu–M distance/pm	349 (427)	410	420	437	312–368
M–O distance/pm	ca. 188 (188)			224	199–203
Eu–O distance/pm	ca. 237 (243)			224	230–351
Eu–O–M angle/ $^\circ$	92 (122)	180	180	154	82–115

\* Bond distances and bond angles are for  $\text{Y}_3\text{Fe}_5\text{O}_{12}$  which has a similar cell dimension. Values in parentheses refer to the third-nearest neighbour  $\text{Fe}^{3+}$  ions.

therefore be taken to be a random solid solution. The replacement of Fe by Cr can be predicted to cause an imbalance in the exchange fields acting on the europium sites and in this way may result in the presence of a significant hyperfine flux density. The probability that  $n$  of the eight nearest neighbour iron sites about each europium site are occupied by Cr is given by  $8!(1-x)^{8-n}x^n/[n!]$  where  $x$  is the fractional occupancy 0.2. Thus 16.8% of the sites will have no chromium neighbours (and therefore no exchange field), 33.6% of the sites will have one, 29.4% two, and 14.7% three. The Fe–Cr exchange is believed<sup>13</sup> to be ferromagnetic, in contrast to the Fe–Fe and Cr–Cr exchange which are antiferromagnetic. The effect will be to cause an imbalance in the exchange interaction at 83% of the  $\text{Eu}^{3+}$  sites which, when coupled with the four different M–M' distances, will result in a wide distribution of values for the effective exchange field. The practical result will be an additional broadening due to the presence of a range of magnetic hyperfine flux densities. The linewidth at 295 K was found to be  $3.75 \text{ mm s}^{-1}$  (as compared to  $3.41 \text{ mm s}^{-1}$  for the pure ceramic phase).

Similar arguments can be applied to  $\text{EuFe}_{0.9}\text{Al}_{0.1}\text{O}_3$ , except that here the substituent is diamagnetic. The linewidths were  $4.01 \text{ mm s}^{-1}$  at 295 K and  $4.62 \text{ mm s}^{-1}$  at 85 K. In this case 43% of the sites have no aluminium neighbours.

derives from the two nearest-neighbour  $\text{Fe}^{3+}$  ions despite the low bond angle ( $92^\circ$ ) for the Eu–O–Fe exchange, and only 12% from the four third-nearest neighbour  $\text{Fe}^{3+}$  ions despite the more favourable bond angle ( $122^\circ$ ). All six of these  $\text{Fe}^{3+}$  ions are in tetrahedral co-ordination to oxygen. Moreover, the exchange from only one iron atom in  $\text{SrEu}_2\text{Fe}_2\text{O}_7$  is comparatively weak despite the wide bond angle, and it has been suggested<sup>3</sup> that this factor is much less important than the longer Fe–O bond distance in this distorted octahedral co-ordination (224 pm) compared with the short Fe–O distance (ca. 188 pm) in  $\text{Eu}_3\text{Fe}_5\text{O}_{12}$ .

Close examination of the  $\text{EuFeO}_3$  structure shows that each of the eight nearest-neighbour iron sites has one exchange path to europium with an Fe–O bond distance of between 199 and 203 pm and a Eu–O bond distance of between 230 and 236 pm with the Eu–O–Fe bond angle between  $91$  and  $115^\circ$  (other exchange paths have much longer bond lengths). It therefore seems likely that the longer Fe–O bond length in  $\text{EuFeO}_3$  has drastically reduced the magnetic exchange interaction, and that in  $\text{SrEu}_2\text{Fe}_2\text{O}_7$  the wider bond angle is important in preserving the exchange with octahedrally co-ordinated  $\text{Fe}^{3+}$  ions.

Although the linewidths of Al-substituted  $\text{EuFeO}_3$  are broader, this does not necessarily signify magnetic exchange. The size difference between  $\text{Al}^{3+}$  and  $\text{Cr}^{3+}$

could result in considerable localised distortions and consequent changes in the quadrupole interaction. Further work is required to clarify this point, and more detailed experiments in  $\text{EuMO}_3$  solid solutions are in progress.

[1/180 Received, 5th February, 1981]

#### REFERENCES

- <sup>1</sup> G. W. Dulancy and A. F. Clifford, 'Mössbauer Effect Methodology,' ed. I. J. Gruverman, Plenum Press, New York, 1970, vol. 5, p. 65.
- <sup>2</sup> T. C. Gibb and R. Greatrex, *J. Solid State Chem.*, 1980, **34**, 279.
- <sup>3</sup> T. C. Gibb, *J. Phys. C*, 1981, **14**, 1985.
- <sup>4</sup> P. K. Gallagher, *Mater. Res. Bull.*, 1968, **3**, 225.
- <sup>5</sup> M. Marezio, J. P. Remeika, and P. D. Dernier, *Acta Crystallogr. Sect. B*, 1970, **26**, 2008.
- <sup>6</sup> R. L. White, *J. Appl. Phys.*, 1969, **40**, 1061.
- <sup>7</sup> D. Treves, *J. Appl. Phys.*, 1965, **36**, 1033.
- <sup>8</sup> M. T. Hutchings and W. P. Wolf, *J. Chem. Phys.*, 1964, **41**, 617.
- <sup>9</sup> R. G. Barnes, R. L. Mössbauer, E. Kankeleit, and J. M. Poindexter, *Phys. Rev. A*, 1964, **136**, 175.
- <sup>10</sup> R. E. Watson and A. J. Freeman, *Phys. Rev. A*, 1964, **135**, 1209.
- <sup>11</sup> A. J. Freeman and R. E. Watson, *Phys. Rev.*, 1962, **127**, 2058.
- <sup>12</sup> M. Stachel, S. Hufner, G. Crecelius, and D. Quitmann, *Phys. Rev.*, 1969, **186**, 355.
- <sup>13</sup> R. P. Gupta and S. K. Sen, *Phys. Rev. Sect. A*, 1973, **7**, 850.
- <sup>14</sup> Y. Nishihara, *J. Phys. Soc. Jpn.*, 1975, **38**, 710.
- <sup>15</sup> I. Nowik and S. Ofer, *Phys. Rev.*, 1967, **153**, 409.